

# Identification of Human Host Proteins Contributing to H5N1 Influenza Virus Propagation by Membrane Proteomics

Cheng Liu,<sup>†,‡,§</sup> Anding Zhang,<sup>†,‡,§</sup> Jing Guo,<sup>‡</sup> Jing Yang,<sup>‡</sup> Hongbo Zhou,<sup>†,‡</sup> Huanchun Chen,<sup>†,‡</sup> and Meilin Jin<sup>†,\*,‡</sup>

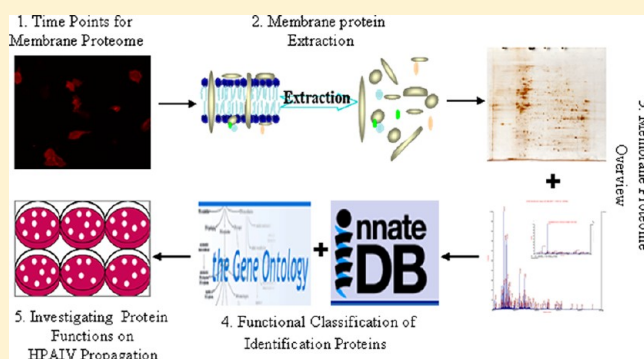
<sup>†</sup>State Key Laboratory of Agricultural Microbiology, Huazhong Agricultural University, Wuhan, Hubei, P. R. China

<sup>‡</sup>College of Veterinary Medicine, Huazhong Agricultural University, Wuhan, Hubei, P.R. China

## S Supporting Information

**ABSTRACT:** The highly pathogenic avian influenza (HPAI) H5N1 virus is a highly virulent pathogen that causes respiratory diseases and death in humans and other animal species worldwide. Because influenza is an enveloped virus, the entry, assembly, and budding of virus particles are essential steps in the viral life cycle, and the virus relies on the participation of host cellular membrane proteins for all of these steps. Thus, we took a comparative membrane proteomics approach by using 2-DE coupled with MALDI-TOF/TOF MS to profile membrane proteins involved in H5N1 virus infection at 6, 12, and 24 h. Forty-two different proteins were found to vary on A549 cells due to H5N1 virus infection. Of these proteins, 57% were membrane or membrane-associated proteins. To further characterize the roles of novel identified proteins in virus propagation, the siRNA technology were applied and complement component C1q binding protein, annexin 2, prohibitin, peroxiredoxin 1 and heat shock protein 90-beta were successfully demonstrated to be contributed to viral propagation. In conclusion, the present study provides important new insight into understanding the roles of host membrane proteins in viral infection progress, and this insight is of particular importance for the development of novel therapeutic strategies.

**KEYWORDS:** HPAI H5N1 virus, proteomics, membrane proteins, viral propagation



## INTRODUCTION

The HPAI H5N1 virus directly transmitted from poultry to humans was first reported in Hong Kong in 1997 and caused a remarkable severe disease in humans with a high mortality up to 60%, which is 100- to 1000-fold higher compared to seasonal influenza viruses.<sup>1</sup> Because influenza is an enveloped virus, infection must begin with the fusion of the virus and the host plasma membrane. Subsequently, the virus particles entry into the host cells through early endosome by endocytosis.<sup>2,3</sup> Finally, virus particles assembled and bud out at the host cell plasma membrane.<sup>4</sup> These steps are critically important for both the survival of the virus and the disease-producing ability of the virus in the host. In these steps, host cellular membrane proteins play essential roles which remain to be elicited.

Genomics and genome-wide RNAi screen have frequently been used to study the cellular proteins involved in the process of influenza infection. For example, microarray technology was used to demonstrate that the pandemic H1N1 virus has the ability to inhibit biological pathways associated with cytokine responses, NK activation and macrophage recognition.<sup>5</sup> A family of antiviral restriction factors, the IFITM proteins that mediate cellular innate immunity to influenza A Virus (IAV), West Nile virus, and Dengue virus, was identified by siRNA

screen.<sup>6</sup> The use of genome microarray may detect all regulation genes, but it is well-known that protein and mRNA levels do not correlate well.

Proteomics combined with bioinformatics has emerged as an important tool to extract detailed information of pathogen–host interactions. Using proteomics approach, a set of cytosolic proteins of primary human airway epithelial cells response to influenza infection were identified.<sup>7</sup> A study on regulation of both antiviral and cell death signals during IAV infection by the interaction between actin network and mitochondria was performed using subcellular proteomic methods.<sup>8</sup> Most proteomics studies have focused on changes in protein expression in whole cell lysates or individual tissues.<sup>7,9,10</sup> Though a few subcellular proteome research have been reported, most of them focused on mitochondrial and nuclear proteome.<sup>8,11,12</sup> Very few researches aimed directly at membrane proteins, which have essential cellular functions, due to the hydrophobic nature of membrane proteins makes them notoriously difficult to study. The use of subcellular proteomics can provide deeper insight into underlying cellular

Received: July 13, 2012

Published: September 17, 2012

functions of proteins in different subcellular compartments, and proteins translocations between different cell compartments can be detected.<sup>13</sup> Thus, an understanding of the membrane proteins involved in influenza virus infection progress by membrane proteomics remains a high priority.

To answer these unresolved questions, we focused on the changes in the levels of membrane proteins, using comparative proteomics to screen for proteins associated with influenza virus production and with the responses of human lung epithelial cells to influenza virus infection. In this study, A549 cells were infected with a HPAI H5N1 virus strain, and the membrane fractions were prepared. These fractions were analyzed by using two-dimensional electrophoresis for protein separation and mass spectrometry for protein identification. We found 42 altered cellular membrane or membrane-associated proteins that were regulated by HPAI H5N1 virus infection, including 16 up-regulated proteins and 26 down-regulated proteins. Especially, five identified cell surface proteins were demonstrated to be associated with viral propagation. These proteins are complement component C1q binding protein (C1QBP) and annexin 2 (ANXA2), which are inhibitors of HPAI H5N1 virus generation; and three proteins that facilitate viral replication, prohibitin (PHB), heat shock protein 90-beta (HSP90AB1) and peroxiredoxin 1 (PRDX1). Our data thus indicate that there are specific functional interactions between HPAI H5N1 virus and the plasma membrane rather than a global change in whole cell lysates integrity.

## MATERIALS AND METHODS

### Cell Cultivation and Virus Infection

Human lung epithelial cell line A549 and MDCK cells were cultured in F12 and DMEM medium (Gibco, Invitrogen), respectively, supplemented with 2 mM L-glutamine, 10 mM HEPES, 1.5 g/L sodium bicarbonate, 4.5 g/L glucose and 10% FBS (Gibco, Invitrogen). For infection, the growth medium was withdrawn and cells were washed three times with PBS before adding serum-free medium containing the virus seed.

The HPAI H5N1 virus strain, A/chicken/Hubei/327/2004(H5N1) (abbreviated as DW), isolated from chicken and conserved by the State Key Laboratory of Agricultural Microbiology, was cultured in MDCK cells and stored at  $-80^{\circ}\text{C}$ . For infection experiments in A549 cells, a multiplicity of infection (MOI) of 0.5 was used. Mock infection performed using the same procedure as for viral infection but without the addition of virus was used as control. The control and viral infection samples were processed identically. All experiments with the H5N1 virus were performed in a Biosafety Level 3 laboratory.

### Photomicrography and Immunofluorescence

The DW-infected and mock-infected A549 cells were carried out in 12-well plates, and the cells were examined microscopically for cytopathic effect (CPE) at 0, 6, 12, 24, 36, and 48 h post infection (hpi). For immunofluorescence analysis (IFA), infected A549 cells in the 12-well plates were washed with PBS and fixed with 4% paraformaldehyde for 15 min at room temperature at the same time points as above. Nonspecific binding sites were blocked with 3% BSA in PBS for 1 h at  $37^{\circ}\text{C}$ . The fixed cells were incubated for 2 h at  $37^{\circ}\text{C}$  with primary antibody (anti-HA) diluted in blocking solution. Cy3-conjugated anti-mouse IgG (ProteinTech) was diluted in blocking solution and incubated with the cells for at least 30 min at  $37^{\circ}\text{C}$ . Cells were washed five times with PBS between

all antibody treatments. Then, the fluorescence was examined microscopically with Olympus  $2\times 70$  and cells were photographed with a DP70 digital camera.

### Protein Extraction

Proteins were extracted at 6, 12, and 24 hpi. Each sample was prepared by lysing approximately  $8.6 \times 10^7$  cells and isolating the membrane fractions with a ProteoExtract Native Membrane Protein Extraction Kit (M-PEK) (Calbiochem) according to the kit instructions with minor modifications. M-PEK is a 2-step native extraction of membrane proteins, which works with low speed centrifugation, and it extracts integral membrane and membrane-associated proteins based on their actual association with cellular membranes. Briefly, the cells were collected using cell scrapers, transferred into appropriate centrifuge tubes and washed three times with wash buffer. Cold extraction buffer I and protease inhibitor cocktail were added to the cells, which were then incubated at  $4^{\circ}\text{C}$ . The insoluble material was precipitated by centrifuge. Cold extraction buffer II and protease inhibitor cocktail were added to the pellet, which was then incubated at  $4^{\circ}\text{C}$  for 30 min. Centrifuge and the supernatant are the membrane fractions enriched in integral membrane and membrane-associated proteins. The protein concentrations were further determined by the 2-D Quant Kit (GE Healthcare).

### 2-DE and Image Analysis

IEF was performed using the IPGphor II system (GE Healthcare) and Immobiline 24-cm DryStrip IPG strips (pH3–10) according to Zou et al.<sup>10</sup> and Zhang et al.<sup>14</sup> The prepared proteins (120  $\mu\text{g}/\text{strip}$ ) were mixed with rehydration buffer (7 M urea, 2 M thiourea, 2% (w/v) CHAPS, 1% (w/v) DTT, 0.5% (v/v) IPG buffer (pH 3–10), 0.002% (w/v) bromophenol blue) and then were focused for a total of 80 kV·h. After IEF, the IPG strips were equilibrated with equilibration buffer (50 mM Tris-HCl, pH 8.8, 6 M urea, 30% (v/v) glycerol, 2% (w/v) SDS, and 0.002% (w/v) bromophenol blue) containing 10 mg/mL DTT for the first step for 15 min, and containing 25 mg/mL iodoacetamide for the second step for a further 15 min. After equilibration, the second-dimension electrophoresis was performed on a 10% SDS polyacrylamide gel using Ettan DALTSix electrophoresis units (GE Healthcare). The proteins were visualized by silver staining. Gel evaluation and data analysis were performed using the ImageMaster v 6.01 program (GE Healthcare). Up-regulated or down-regulated protein spots were defined as spots with the percentage volume (% vol) change greater than 2-fold and a *p*-value of less than 0.05. Three biological repeats were performed for each sample to minimize gel-to-gel variation.

### In-Gel Digestion of Proteins

The protein spots were excised from the silver-stained gels using a 1 mm diameter micropipet tip. The gel pieces were destained for 1 h with 50  $\mu\text{L}$  of 30 mmol/L  $\text{K}_3\text{Fe}(\text{CN})_6$  and 100 mmol/L  $\text{Na}_2\text{S}_2\text{O}_3$  in a ratio of 1:1 at ambient temperature, and then lyophilized. The dried gel particles were reswollen with 5  $\mu\text{L}$  of 25 mM ammonium bicarbonate containing 10 ng of trypsin (Promega) at  $4^{\circ}\text{C}$  for 30 min. In-gel tryptic digestion was performed overnight at  $37^{\circ}\text{C}$ . After tryptic digestion, the peptide mixtures were mixed with 60% acetonitrile (ACN) and 0.1% TFA, and sonicated for 15 min. The pooled extracts were lyophilized and reconstituted in 20% ACN (Merck) prior to MALDI-TOF/TOF MS analysis. The

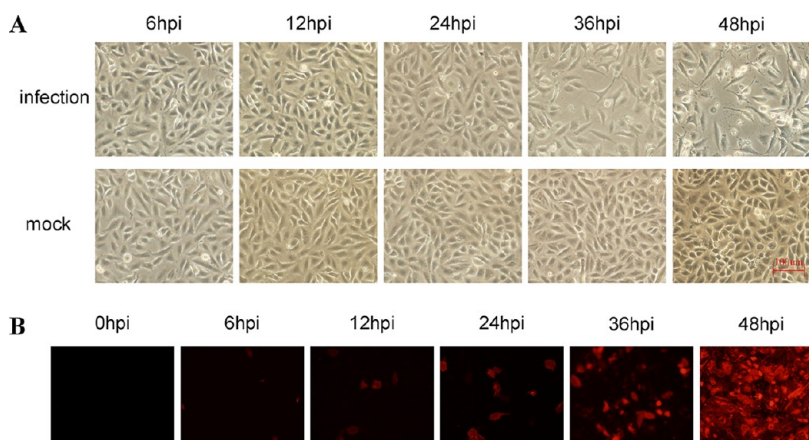


**Figure 1.** Kinetics of influenza infection in cultured A549 cells. (A) Photomicrographs of A549 cells infected with DW at MOI = 0.5 PFU/cell (top), and mock-infected cells (bottom) taken at the indicated time points post infection (indicated at the top). Scale bar = 100  $\mu$ m. (B) Indirect immunofluorescence microscopy analysis of influenza virus propagation in A549 cells.

matrix used was a 5 mg/mL solution which dissolving  $\alpha$ -cyano-4-hydroxycinnamic acid (Sigma) in 50% ACN and 0.1% TFA (Merck).

#### MALDI-TOF/TOF MS Analysis and Database Search

The mass spectra were obtained using a 4800 Plus MALDI TOF/TOF Analyzer (Applied Biosystems, Foster City, CA) in positive ion reflector mode. The Nd:YAG laser was operated at a wavelength of 355 nm with an acceleration voltage of 2 kV. The PMF mass range was 800–4000 Da. In each MS spectrum, the eight most abundant MS peaks were selected for MS/MS using an acquisition method that excluded ions with S/N less than 50. Database searches were performed with MASCOT 2.1 software (Matrix Science, London, U.K.) against the NCBI nr and IPI\_human database. The search parameters were the following: carbamidomethyl cysteine as fixed modification by the treatment with iodoacetamide, oxidized methionines as variable modification, peptide charge state as 1+ and 1 missed cleavage site allowed. Peptide and fragment mass tolerance were set to  $\pm 100$  ppm and  $\pm 0.8$  Da, respectively. MASCOT protein scores of greater than 55 were considered statistically significant ( $p < 0.05$ ). The functional classification and cellular localization of the identified cellular proteins was performed using the gene ontology (GO) and InnateDB (<http://www.innatedb.ca/>).

#### Western Blot Analysis

To further confirm the alterations of membrane-association protein expression during DW infection, isolated membrane proteins from DW-infected and mock-infected A549 cells were dissolved in SDS sample buffer (250 mM Tris-HCl, pH 6.8; 20% glycerol; 4% SDS; 0.2% bromophenol blue) and heated at 95  $^{\circ}$ C for 5 min. Equal amounts of protein (30  $\mu$ g) from each sample were loaded into 12% SDS-PAGE gels and transferred onto nitrocellulose membranes (Millipore). Membranes were blocked with 3% BSA, stained with different primary antibodies overnight, washed three times, incubated with secondary antibodies for 1 h, then, washed another five times and detected by ECL. The primary antibodies used in this study were antibodies against GAPDH (CWBIO); C1QBP and integrin alpha 3 (ITGA3) (Millipore); annexin A1 (ANXA1), HSP90AB1, and vimentin (VIM) (Epitomics); and ANXA2, enolase 1 (ENO1), PRDX1, heterogeneous nuclear ribonucleoprotein K (HNRNPK), cadherin, and PHB (ProteinTech). The secondary antibodies used in this study were horseradish peroxidase (HRP)-conjugated anti-mouse IgG or HRP-

conjugated anti-rabbit IgG (SouthernBiotech). The GAPDH protein was used as a control.

#### Small Interference RNA (siRNA) Experiments for Viral Propagation Analysis

All siRNA duplexes were purchased from GenePharma and resuspended in diethyl pyrocarbonate-treated water to a final storage concentration of 20  $\mu$ M. The effective siRNA duplexes sequences are listed in Supplementary Table 1 (Supporting Information). A549 cells were transfected with either scrambled (control) or gene specific siRNA using HiPerFect Transfection Reagent (Qiagen) according to the manufacturer's instruction. Thirty-six hours after transfection, cells were infected with DW at a MOI of 0.1. Twenty-four hours post infection, the cell culture supernatants were collected for plaque assays, and the total proteins and the total RNA of the cells were isolated for Western blot and quantitative real-time PCR (qRT-PCR) analyses, respectively, to confirm the efficiency of the siRNAs.

#### RNA Extraction and qRT-PCR

Specific primers for the target genes were designed by Primer 5.0 based on the corresponding gene sequences of the identified proteins (Supplementary Table 2, Supporting Information). To confirm the efficiency of the siRNA, the total cellular RNA was extracted with TRIzol Reagent (Invitrogen) 36 h after transfection. RNA concentrations were measured with a spectrophotometer (OD260/OD280). The reverse transcription was performed using oligo(dT) as the primer. After the RNA was reverse-transcribed to cDNA, the qRT-PCR assays was performed using an Applied Biosystems 7500 Real-time PCR System in a 20  $\mu$ L volume containing 100 ng of the cDNA template, FastStart DNA Master SYBR Green I Mix reagent kit (Roche) and 200 nM of each primer. After predenaturation at 95  $^{\circ}$ C for 5 min, amplification was performed for 45 cycles, each consisting of 95  $^{\circ}$ C for 30 s, 56  $^{\circ}$ C for 30 s, and 72  $^{\circ}$ C for 30 s. Melting curves were obtained, and a quantitative analysis of the data was performed using the 7500 System SDS software v1.3.1 in a relative quantification (ddCt) study model (Applied Biosystems).

#### Virus Titer Determination Using Plaque Assays

Confluent monolayers of MDCK cells in six-well plates were washed with DMEM and infected with serial 10-fold dilutions of supernatant from the infected cells for 1 h. After incubation with virus, the cells were washed with DMEM and overlaid with

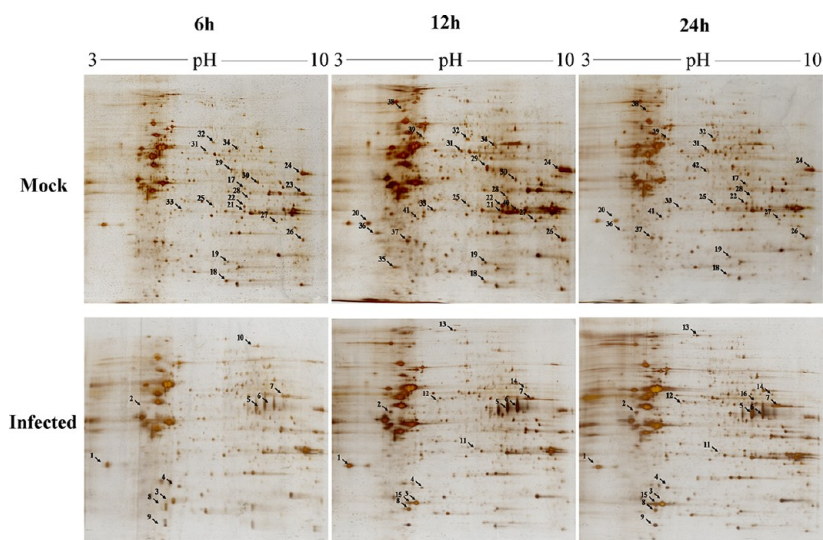


**Figure 2.** Representative 2-D gels for the membrane fractions of DW-infected and mock-infected A549 cells. The proteins (120  $\mu$ g) were first separated in a linear gradient of pH 3–10, followed by separation in 10% SDS-PAGE gels. These gels were stained with silver. Numbers 1–42 mean the protein spots number. Protein functions are listed in Table 1 with corresponding numbers.

1.6% low-melting-temperature agarose (Amresco), mixed in a 1:1 ratio with 2 $\times$  DEME medium without phenolsulfonphthalein (Hyclone) containing 3.7 g/L sodium bicarbonate (Amresco). Virus plaques were stained with 0.01% toluylene red (Amresco). Virus plaques were counted and viral titers were calculated after three days of incubation at 37  $^{\circ}$ C in 5% CO<sub>2</sub>. All data were expressed as the mean of triplicate samples.

#### Statistical Analysis

All assays were performed in triplicate. The data were analyzed using a two-tailed paired Student's *t* test, and values with *p* < 0.05 were considered to be significant.

## RESULTS AND DISCUSSION

### Characteristics of HPAI H5N1 Virus Infection Kinetics in Cultured A549 Cells

For a better understanding of the influenza viral infection process, cultured A549 cells were infected with the influenza strain DW and microscopically monitored for cytopathic effects (CPE) at 6, 12, 24, 36, and 48 hpi. To find a gradually infection process in A549 cells, we used a low dose (MOI = 0.5) as the infection dose in this research, because when we used high infection dose (MOI = 1 and 2) of this HPAI H5N1 virus, the cells decrease rapidly and evident CPE can be detected, which could lead to the identification of a large number of death associated proteins. Cells infected with DW and cultured for 24 h or less showed no detectable CPE. Up to 36 hpi, minimal CPE was detected (Figure 1A). The viral propagation was detected at 6 hpi and readily apparent at later time points by IFA with antibody against HA (Figure 1B). To identify membrane proteins involved in the early response to infection, those time points at which the virus propagated effectively with no significant CPE, that is, 6, 12, and 24 hpi, were selected for the subsequently membrane proteome study.

### Membrane Proteome Overview of the Effects of HPAI H5N1 Virus Infection on A549 Cells

For membrane proteome analysis, DW-infected and mock-infected A549 cells were harvested at 6, 12, and 24 hpi. The proteins were extracted by the M-PEK and validated to be enrichment membrane proteins by membrane marker (cadher-

in) in Supplementary Figure 1 (Supporting Information), and subsequently separated using 2-DE technology. Comparative analysis of the 2-DE gels revealed 20 clearly up-regulated and 36 down-regulated protein spots (threshold greater than 2-fold, *p* < 0.05) (Figure 2). The differentially regulated protein spots are marked in the images and displayed in Supplementary Figure 2 (Supporting Information) in enlarged form. To identify these proteins in the 2-DE gels, the marked spots were excised and subjected to MALDI-TOF/TOF MS analysis. In all, 42 altered protein spots were successfully identified, including 16 up-regulated and 26 down-regulated (Table 1). We found that host proteins are more likely to be down-regulated by influenza viral infection in the present research. It may be because that our research was a subcellular proteome research, which specially aimed at the membrane fractions of cells. Membrane or membrane associated proteins were down-regulated perhaps caused by influenza infection processes, such as endocytosis. A complete list of all proteins and peptides identified in this study is presented in Supplementary Table 3 (Supporting Information). Of these proteins, 57% are membrane proteins or membrane-associated proteins. The remaining proteins were predicted to localize to the cytoplasm, mitochondrial and nucleus (Table 1), and many of these proteins were detected previously in the other membrane proteome studies.<sup>15,16</sup> To confirm the altered of the identified membrane proteins, nine randomly selected proteins were subjected to Western blot analysis with specific antibodies. All nine proteins showed alter expression corresponding to the membrane proteome analysis, indicating that the identified proteins were regulated by influenza virus (Figure 3).

### Characterization of the Differentially Regulated Proteins Identified in the Membrane Proteome

Classification of the subcellular localizations of 42 proteins based on annotations in the Gene Ontology Consortium and InnateDB (<http://www.innatedb.ca/>) revealed several classes of enriched proteins. Fifty-seven percent are known or predicted membrane proteins, or proteins known to interact with other membrane proteins. Twenty-seven percent are cytoplasmic, 9% are associated with the nucleus. These identified proteins in multicompartment can engage in different

Table 1. Summary of Identification Results from the Altered Proteins in the Membrane Fractions of DW-Infected A549 Cells

spot ID <sup>a</sup>	protein name	abbr.	biologic function <sup>b</sup>	subcellular localization <sup>c</sup>	variation <sup>d</sup>		
					6 hpi	12 hpi	24 hpi
Viral Proteins							
3	nonstructural protein 1 [Influenza A virus (A/chicken/Hubei/327/2004(H5N1))]	NS1	Influenza nonstructural protein		↑	↑	↑
8	nonstructural protein 1 [Influenza A virus (A/chicken/Hubei/327/2004(H5N1))]	NS1	Influenza nonstructural protein		↑	↑	↑
15	nonstructural protein 1 [Influenza A virus (A/chicken/Hubei/327/2004(H5N1))]	NS1	Influenza nonstructural protein		↑	↑	↑
5	hemagglutinin [Influenza A virus (A/chicken/Hubei/14/2004(H5N1))]	HA	Envelope protein of influenza virus mediates viral entry		↑	↑	↑
6	hemagglutinin [Influenza A virus (A/chicken/Thailand/Sukhothai-01/2004(H5N1))]	HA	Envelope protein of influenza virus mediates viral entry		↑	↑	↑
Cytoskeleton/Structural Proteins							
2	Vimentin	VIM	Intermediate filament protein	cytoskeleton	↑	↑	↑
14	keratin, type II cytoskeletal 2 epidermal	KRT2	Structural constituent of cytoskeleton	cytoskeleton membrane		↑	↑
16	epidermal cytokeratin 2	KRT2	Structural constituent of cytoskeleton	cytoskeleton membrane			↑
41	Keratin, type I cytoskeletal 10	KRT10	Structural constituent of epidermis	Intermediate filament membrane			↓
24	Keratin, type II cytoskeletal 1	KRT1	Receptor activity; Structural constituent of cytoskeleton	Cell membrane	↓	↓	↓
36	Keratin, type I cytoskeletal 9	KRT9	Structural constituent of cytoskeleton	Cytoskeleton; Membrane		↓	↓
25	annexin A1	ANXA1	Receptor binding; Structural molecule activity; Calcium-dependent phospholipid binding	Cell membrane; Cytoplasm	↓	↓	↓
27	annexin A2, isoform CRA_c	ANXA2	Calcium ion binding; Calcium-dependent phospholipid binding; Cytoskeletal protein binding	Basement membrane; Cytoplasm	↓	↓	↓
Cellular Signal Transduction Proteins							
13	integrin alpha 3	ITGA3	cell adhesion and interaction integrin-mediated signaling pathway	Membrane		↑	↑
4	prohibitin	PHB	negative regulation of cell proliferation	Membrane	↑	↑	↑
37	cathepsin D	CTSD	response to biotic stimulus	Membrane		↓	↓
35	Translationally controlled tumor protein	TPT1	calcium ion binding regulation of apoptosis	Cytoplasm		↓	
29	Chain A, Crystal Structure Of Human Enolase 1	ENO1	Glycolysis Magnesium ion binding	Cytoplasm; Cell membrane	↓	↓	
Transcription/RNA Processing							
11	heterogeneous nuclear ribonucleoprotein D-like	HNRPDL	Regulation of transcription RNA processing	Nucleus; Cytoplasm		↑	↑
32	heterogeneous nuclear ribonucleoprotein L, isoform CRA_a	HNRNPL	Nuclear mRNA splicing, via spliceosome potassium ion transport	Nucleus nucleoplasm	↓	↓	↓
39	heterogeneous nuclear ribonucleoprotein K	HNRNPK	Nuclear mRNA splicing, via spliceosome signal transduction RNA splicing	Cytoplasm; Nucleus nucleoplasm		↓	↓
42	Eukaryotic initiation factor 4A-III	EIF4A3	Nuclear-transcribed mRNA catabolic process RNA splicing	Nucleus			↓
Immune Response							
1	complement component 1, q subcomponent binding protein	C1QBP	Complement component C1q binding; Innate immune response	Mitochondrion matrix; Plasma membrane	↑	↑	↑
20	complement component 1, q subcomponent binding protein	C1QBP	Complement component C1q binding; Innate immune response	Mitochondrion matrix; Plasma membrane		↓	↓
Stress Response/Molecular Chaperone							
18	peroxiredoxin 1	PRDX1	Oxidative stress response	Cytoplasm; Membrane	↓	↓	↓
38	heat shock protein HSP 90-beta	HSP90AB1	Molecular chaperone	Cytoplasm		↓	↓
Metabolism							
12	dihydrolipoamide succinyltransferase	DLST	Acyltransferase activity	Mitochondrion		↑	↑
28	Transketolase	TKT	transketolase activity	Cytoplasm	↓	↓	↓
10	Aconitase 2	ACO2	Aconitate hydratase activity	Mitochondrion	↑		
30	citrate synthase	CS	Citrate (Si)-synthase activity	Mitochondrion matrix	↓	↓	
31	aldehyde dehydrogenase 1A1 isoform 6	ALDH1A1	Aldehyde dehydrogenase (NAD) activity; Ras GTPase activator activity	Cytoplasm	↓	↓	↓
21	aldo-keto reductase family 1 member B10	AKR1B10	Aldo-keto reductase activity; Oxidoreductase activity	Cytoplasm	↓	↓	
40	Aldo-keto reductase family 1 member B10	AKR1B10	Aldo-keto reductase activity; Oxidoreductase activity	Cytoplasm		↓	
22	aldo-keto reductase family 1 member C2 isoform 1	AKR1C2	3-alpha-hydroxysteroid dehydrogenase (A-specific) activity	Cytoplasm	↓	↓	↓
19	triosephosphate isomerase isoform 2	TPII	Triose-phosphate isomerase activity	cytosol	↓	↓	↓

Table 1. continued

spot ID <sup>a</sup>	protein name	abbr.	biologic function <sup>b</sup>	subcellular localization <sup>c</sup>	variation <sup>d</sup>		
					6 hpi	12 hpi	24 hpi
Metabolism							
23	aspartate aminotransferase, mitochondrial	GOT2	L-aspartate:2-oxoglutarate aminotransferase activity	Mitochondrion matrix; Cell membrane	↓		
34	UDP-glucose 6-dehydrogenase	UGDH	UDP-glucose 6-dehydrogenase activity	Nucleus		↓	
33	L-lactate dehydrogenase B chain	LDHB	L-lactate dehydrogenase activity	Cytoplasm	↓	↓	↓
17	Trifunctional enzyme subunit alpha	HADHA	Acyl-CoA binding	Mitochondrion; Mitochondrial inner membrane	↓		
26	NAD(P)H dehydrogenase [quinone] 1 isoform c	NQO1	NAD(P)H dehydrogenase (quinone) activity	Cytoplasm	↓	↓	↓
9	ATP synthase subunit d	ATP5H	hydrogen ion transmembrane transporter activity ATPase activity	Mitochondrion inner membrane	↑		↑
7	ATP synthase, H <sup>+</sup> transporting, mitochondrial F1 complex, alpha subunit 1	ATP5A1	hydrogen ion transporting ATP synthase activity, rotational mechanism	Mitochondrion inner membrane	↑	↑	↑

<sup>a</sup>Spot ID represents the protein spot number on the 2-DE gels. <sup>b,c</sup>Functions (<sup>b</sup>) and subcellular localization (<sup>c</sup>) of identified proteins was performed using the gene ontology (GO) and InnateDB (<http://www.innatedb.ca/>). <sup>d</sup>The arrow “↑” represents the proteins we identified were up-regulated in this membrane proteomic research at the corresponding time point and the arrow “↓” represents the identified proteins were down-regulated.

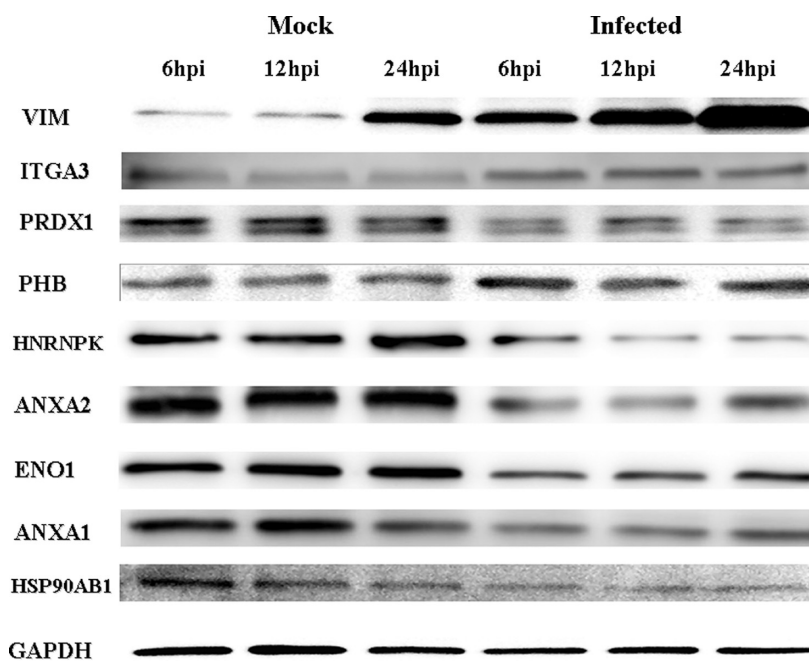


**Figure 3.** Western blot confirming representative proteins in HPAI H5N1 virus infected A549 cells. Membrane fractions were prepared from A549 cells that were either mock-infected or DW-infected for different time periods. An equal amount of protein (30  $\mu$ g) from each sample was used for the Western blot analysis. The GAPDH protein was used as a control.

cellular processes, including cytoskeletal components; cell adhesion and interaction; cellular signal transduction; immune response; stress response; transcription/RNA processing and metabolism. Besides, two influenza proteins, HA and NS1, were successfully identified in the A549 infected cells (Table 1). NS1 is a highly abundant protein in infected cells and has multifunctions that participate in both protein–protein and protein–RNA interactions. So, the NS1 protein was brought to the cell membrane maybe through the interactions with host cell membrane or membrane-associated proteins, such as PI3K p85beta.<sup>17,18</sup> HA is a membrane protein of the influenza virus, which can express on the membrane of the infected cells. However, influenza virus has three membrane proteins (HA, NA and M2). We have not detected the NA and M2 may be due to that proteins which could be analyzed by 2-DE have

limits on isoelectric point, molecular mass and abundance. This was supported by other proteome studies of influenza virus-infected, which could not identify any viral proteins.<sup>19,20</sup>

In this study, we present for the first time a global view of the dynamic changes undergone by the A549 cells membrane proteome during HPAI H5N1 virus infection. Our study reveals several new surface proteins that may play important roles in influenza virus life cycle and host cellular pathophysiological processes against the virus infection. ITGA3 (spot 13), a member of the integrins, was found to be up-regulated from 12 to 24 hpi (Table 1 and Supplementary Figure 2, Supporting Information). Two annexins, ANXA1 (spot 25) and ANXA2 (spot 27), were found to be down-regulated after HPAI H5N1 virus infection (Table 1 and Supplementary Figure 2, Supporting Information). These proteins have relevant

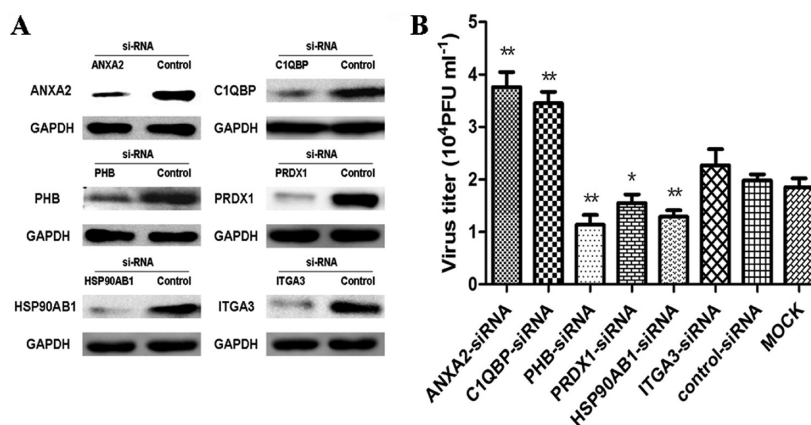


**Figure 4.** Identified host proteins contributing to viral propagation. (A) The efficiency of the specific siRNAs. Transfection of A549 cells with gene-specific and nontargeting control siRNAs. Sixty hours after transfection, the total cellular protein was analyzed by Western blotting. GAPDH served as protein loading control. (B) Effects of six chosen proteins on viral propagation. A549 cells were transfected with the indicated siRNAs, Thirty-six hours after transfection, cells were infected with DW at MOI of 0.1. Twenty-four hours after infection, supernatants were harvested and the virus titers were determined by standard plaque assays. Bars represent the mean  $\pm$  SD ( $n = 3$ ), \* $p < 0.05$  and \*\* $p < 0.01$ .

functions in membrane/protein transport and in endocytosis.<sup>21,22</sup> Also, several multifunctional, multicompartiment cellular proteins, such as PHB (spot 4), C1QBP (spot 1 and 20), and PRDX1 (spot 18) (Table 1 and Supplementary Figure 2, Supporting Information), were found altered in the membrane fraction after HPAI H5N1 virus infection. Most of these membrane proteins have never been identified previously in influenza infected host cells using the whole-cellular proteomics.

Several proteins identified in the present study were extremely associated with influenza infection. Cytoskeletal proteins changed dramatically after HPAI H5N1 virus infection (Table 1). It has been reported that cytoskeleton and cytoskeleton-associated complexes in host cells provided numerous support functions for viral gene expression to allow the viral infectious cycle.<sup>23</sup> Three hnRNPs identified in this membrane proteomics study, including two down-regulated (spots 32 and 39) and one up-regulated (spot 11) (Table 1 and Supplementary Figure 2, Supporting Information), have been suggested to have an important role in influenza virus gene expression.<sup>24</sup> The hnRNPs are RNA binding proteins and form complexes with heterogeneous nuclear RNA (hnRNA). These proteins participate directly or indirectly in the processing of pre-mRNAs into mature mRNAs and in other aspects of mRNA metabolism and transport.<sup>25,26</sup> Among the three hnRNPs, HNRNPK (spot 39) was identified as important for viral infection, RNA transcription and replication steps of influenza viral life cycle.<sup>27,28</sup> We also identified a heat shock protein, HSP90AB1 (spot 38) (Table 1), which has been reported to be involved in influenza virus RNA synthesis.<sup>29</sup>

Through this membrane proteomics analysis, we found that a set of membrane or membrane-associated proteins in the host cells was largely altered when suffering from the HPAI H5N1 virus infection. Especially, several typically low-abundance membrane proteins were novelly identified using this approach. These proteins may have underlying cellular functions that extremely participate in the influenza virus life cycle, which remain to be clarified.

#### Identification of Host Proteins Contributing to Viral Propagation

During influenza virus infection, the virus utilizes the host cellular machinery to complete its life cycle. To investigate the

biological effect of our identified proteins, the roles of six proteins in virus propagation were analyzed by siRNA. The expression of these proteins was substantially inhibited in cells transfected with specific siRNA which was confirmed by Western blotting (Figure 4A) and qRT-PCR (Supplementary Figure 3, Supporting Information). The viral titers in the supernatants were significantly reduced when PHB, PRDX1 and HSP90AB1 were silenced relative to the control ( $p < 0.05$ ). Moreover, knocking-down endogenous ANXA2 or C1QBP in A549 cells favored the propagation of HPAI H5N1 virus. However, treatment with siRNA targeting ITGA3 did not result in a significant difference relative to the control (Figure 4B).

The protein spots numbered 1 and 20 were identified to be the same protein with different isoelectric point, and show different regulated tendencies upon DW infection in A549 cells. From 6 to 24 hpi, protein spot 20 was down-regulated, whereas the more acidic protein spot 1 was up-regulated (Supplementary Figure 2, Supporting Information). Actually, various proteins are identified in more than one spot on the gel, indicating that some regulated proteins had post-translational modifications, including phosphorylation, acetylation, and so forth.<sup>30</sup> C1QBP is a biologically important, multifunctional, multicompartiment cellular protein that plays an important role in infection, inflammation, cancer and autoimmunity.<sup>31</sup> It has been reported to be phosphorylation on the cell surface.<sup>32</sup> The up-regulated of the more acidic protein spot 1 (C1QBP) may be an enhanced phosphorylation of C1QBP in influenza infected A549 cells, indicating a modification step played roles in cellular signaling and transformation induced by influenza infection rather than an increased protein synthesis. The significance of this change in influenza infection process is worth to be clarified in further studies. Silencing the expression of C1QBP resulted in a higher virus titer than the control (Figure 4B), suggesting that C1QBP may play important roles in the pathogenesis of influenza virus, in the host immunity response and in the defense against viral infection. This protein can therefore be explored as a new therapeutic target. C1QBP was first characterized as a receptor for the globular heads of C1q (gC1q)<sup>33</sup> and it has been reported to recognize and bind to a number of functional antigens of viral origin, including HCV core protein,<sup>34,35</sup> HIV-1 Tat<sup>36</sup> and Rev,<sup>37</sup> core protein V of adenovirus,<sup>38</sup> and Rubella Virus Capsid,<sup>39</sup> demonstrating that

C1QBP plays a crucial role in infection by various pathogenic viruses.

PHB is a ubiquitously expressed membrane proteins and plays various roles in different cellular compartments,<sup>40,41</sup> involving in the essential roles in PI3K/Akt<sup>42</sup> and Ras/MAPK/ERK<sup>43</sup> signaling transduction pathways. PHB has already been reported as a receptor protein mediating DENV-2 entry into insect cells<sup>44</sup> and is up-regulated in cells expressing HCV core protein.<sup>45</sup> In our present study, the PHB protein was up-regulated after influenza infection (Supplementary Figure 2, Supporting Information), similar to the reported in the study of influenza H9N2 infection in ASG cells.<sup>19</sup> Meanwhile, we found that the virus titer was degraded in the PHB silenced A549 cells (Figure 4B), suggesting that PHB may play important roles in the host response or in the life cycle of influenza virus, and implying that appropriate depress the expression of PHB may resist virus infection.

PRDX1 is a member of the peroxiredoxin family of antioxidant enzymes. It is locally inactivated to promote H<sub>2</sub>O<sub>2</sub>-mediated signaling on cell membrane to play an antioxidant protective role in cells.<sup>46</sup> In this study, PRDX1 was down-regulated in the membrane fractions of HPAI H5N1 virus infected A549 cells (Supplementary Figure 2, Supporting Information), while stress proteins are mostly to be up-regulated during viral infection. Further study found that PRDX1 did not show obvious variance in the whole cell lysates after influenza virus infection (Supplementary Figure 4, Supporting Information), implying that it may play other potential cellular functions on membrane compartment in influenza life cycle. The silencing of PRDX1 induced the inhibition of virus propagation (Figure 4B), indicating that PRDX1 may play important roles in the life cycle of influenza virus. PRDX1 has been reported to be one of the inherent host factors implicated in MeV RNA synthesis,<sup>47</sup> and it plays role in protection of respiratory syncytial virus-induced cysteinyl oxidation of nuclear cytoskeletal proteins.<sup>48</sup>

ANXA2 and HSP90AB1 have been reported to participate in the IAV–host interaction.<sup>9,49</sup> ANXA2 can be incorporated into the IAV particles and supports virus replication by converting plasminogen into plasmin, which can serve as an alternative protease for the cleavage of the hemagglutinin (HA) outside of the respiratory tract.<sup>50–52</sup> In this study, ANXA2 was found to be down-regulated during HPAI H5N1 virus infection (Supplementary Figure 2, Supporting Information). Silenced ANXA2 expression can promote the propagation of HPAI H5N1 virus in A549 cells (Figure 4B); this result differs slightly from the results obtained in the study by LeBouder et al.,<sup>51,52</sup> implying that ANXA2 may participate in other important processes in the IAV life cycle, which need further studies. Another protein, HSP90AB1, was also found to be down-regulated after HPAI H5N1 virus infection in the membrane fractions (Supplementary Figure 2, Supporting Information), which is different from the changes in the whole cell lysates (Supplementary Figure 4, Supporting Information) and other whole-cellular proteomics researches,<sup>27,53</sup> implying that it may play an underlying function in membrane compartment response to influenza virus infection. HSP90 has been reported to be involved in the assembly and nuclear transport of the influenza virus RNA polymerase subunits by binding to the PB1 and PB2 polymerase subunits.<sup>29</sup> We demonstrated that the inhibition of HSP90 activity using special siRNA results in decreased influenza propagation (Figure 4B), which corre-

sponds to the results of a study that used HSP90 specific inhibitors.<sup>54</sup>

The present study clearly demonstrates the effects of C1QBP, ANXA2, PHB, PRDX1, and HSP90AB1 on the propagation of HPAI H5N1 virus. These proteins can potentially be developed as targets for future antiviral drugs and vaccines. Further studies to test the functional significance of these proteins remain to be clarified.

## CONCLUSIONS

This membrane proteomics study provided important new insight for understanding the roles of membrane proteins in influenza viral infection progress. Comparing infected A549 cells with the mock-infected A549 cells, 42 altered membrane or membrane-associated proteins were identified, of which five membrane proteins were confirmed to be contributing to HPAI H5N1 virus propagation. These proteins participated in pathways that are important for antiviral or anti-inflammatory responses. Targeting these proteins or the associated pathways in infected cells will favor the development of novel antiviral therapies. Above all, our data represent a valuable source of knowledge about the membrane proteome of HPAI H5N1 virus infected A549 cells.

## ASSOCIATED CONTENT

### Supporting Information

Supplementary Figures 1–4 and Tables 1–3 as noted in text. This material is available free of charge via the Internet at <http://pubs.acs.org>.

## AUTHOR INFORMATION

### Corresponding Author

\*Phone: +86-27-87286905. Fax: +86-27-87282608. E-mail: [jinmeilin@mail.hzau.edu.cn](mailto:jinmeilin@mail.hzau.edu.cn).

### Author Contributions

<sup>§</sup>These authors contributed equally to this article.

### Notes

The authors declare no competing financial interest.

## ACKNOWLEDGMENTS

This work was supported by the National Basic Research Program of China (program 973, 2011CB505004) and National Natural Science Foundation of China (No. 31072154).

## REFERENCES

- (1) Claas, E. C.; Osterhaus, A. D.; van Beek, R.; De Jong, J. C.; Rimmelzwaan, G. F.; Senne, D. A.; Krauss, S.; Shortridge, K. F.; Webster, R. G. Human influenza A H5N1 virus related to a highly pathogenic avian influenza virus. *Lancet* **1998**, *351* (9101), 472–7.
- (2) Samji, T. Influenza A: Understanding the viral life cycle. *Yale J. Biol. Med.* **2009**, *82* (4), 153–9.
- (3) White, J. M. Viral and cellular membrane fusion proteins. *Annu. Rev. Physiol.* **1990**, *52*, 675–97.
- (4) Rossman, J. S.; Lamb, R. A. Influenza virus assembly and budding. *Virology* **2011**, *411* (2), 229–36.
- (5) Yang, X. X.; Du, N.; Zhou, J. F.; Li, Z.; Wang, M.; Guo, J. F.; Wang, D. Y.; Shu, Y. L. Gene expression profiles comparison between 2009 pandemic and seasonal H1N1 influenza viruses in A549 cells. *Biomed. Environ. Sci.* **2010**, *23* (4), 259–66.
- (6) Brass, A. L.; Huang, I. C.; Benita, Y.; John, S. P.; Krishnan, M. N.; Feeley, E. M.; Ryan, B. J.; Weyer, J. L.; van der Weyden, L.; Fikrig, E.;



Adams, D. J.; Xavier, R. J.; Farzan, M.; Elledge, S. J. The IFITM proteins mediate cellular resistance to influenza A H1N1 virus, West Nile virus, and dengue virus. *Cell* **2009**, *139* (7), 1243–54.

(7) Kroeker, A. L.; Ezzati, P.; Halayko, A. J.; Coombs, K. M. Response of primary human airway epithelial cells to influenza infection: a quantitative proteomic study. *J. Proteome Res.* **2012**, *11* (8), 4132–46.

(8) Ohman, T.; Rintahaka, J.; Kalkkinen, N.; Matikainen, S.; Nyman, T. A. Actin and RIG-I/MAVS signaling components translocate to mitochondria upon influenza A virus infection of human primary macrophages. *J. Immunol.* **2009**, *182* (9), 5682–92.

(9) Zhu, J.; Zou, W.; Jia, G.; Zhou, H.; Hu, Y.; Peng, M.; Chen, H.; Jin, M. Analysis of cellular proteome alterations in porcine alveolar macrophage cells infected with 2009 (H1N1) and classical swine H1N1 influenza viruses. *J. Proteomics* **2011**, *75* (6), 1732–41.

(10) Zou, W.; Ke, J.; Zhang, A.; Zhou, M.; Liao, Y.; Zhu, J.; Zhou, H.; Tu, J.; Chen, H.; Jin, M. Proteomics analysis of differential expression of chicken brain tissue proteins in response to the neurovirulent H5N1 avian influenza virus infection. *J. Proteome Res.* **2010**, *9* (8), 3789–98.

(11) Lietzen, N.; Ohman, T.; Rintahaka, J.; Julkunen, I.; Aittokallio, T.; Matikainen, S.; Nyman, T. A. Quantitative subcellular proteome and secretome profiling of influenza A virus-infected human primary macrophages. *PLoS Pathog.* **2011**, *7* (5), e1001340.

(12) Emmott, E.; Wise, H.; Loucaides, E. M.; Matthews, D. A.; Digard, P.; Hiscox, J. A. Quantitative proteomics using SILAC coupled to LC-MS/MS reveals changes in the nucleolar proteome in influenza A virus-infected cells. *J. Proteome Res.* **2010**, *9* (10), 5335–45.

(13) Qattan, A. T.; Mulvey, C.; Crawford, M.; Natale, D. A.; Godovac-Zimmermann, J. Quantitative organelle proteomics of MCF-7 breast cancer cells reveals multiple subcellular locations for proteins in cellular functional processes. *J. Proteome Res.* **2010**, *9* (1), 495–508.

(14) Zhang, A.; Xie, C.; Chen, H.; Jin, M. Identification of immunogenic cell wall-associated proteins of *Streptococcus suis* serotype 2. *Proteomics* **2008**, *8* (17), 3506–15.

(15) Foster, L. J.; Zeemann, P. A.; Li, C.; Mann, M.; Jensen, O. N.; Kassem, M. Differential expression profiling of membrane proteins by quantitative proteomics in a human mesenchymal stem cell line undergoing osteoblast differentiation. *Stem Cells* **2005**, *23* (9), 1367–77.

(16) Berro, R.; de la Fuente, C.; Klase, Z.; Kehn, K.; Parvin, L.; Pumfery, A.; Agbottah, E.; Vertes, A.; Nekhai, S.; Kashanchi, F. Identifying the membrane proteome of HIV-1 latently infected cells. *J. Biol. Chem.* **2007**, *282* (11), 8207–18.

(17) Shin, Y. K.; Liu, Q.; Tikoo, S. K.; Babiuk, L. A.; Zhou, Y. Influenza A virus NS1 protein activates the phosphatidylinositol 3-kinase (PI3K)/Akt pathway by direct interaction with the p85 subunit of PI3K. *J. Gen. Virol.* **2007**, *88* (Pt 1), 13–8.

(18) Li, Y.; Anderson, D. H.; Liu, Q.; Zhou, Y. Mechanism of influenza A virus NS1 protein interaction with the p85beta, but not the p85alpha, subunit of phosphatidylinositol 3-kinase (PI3K) and up-regulation of PI3K activity. *J. Biol. Chem.* **2008**, *283* (34), 23397–409.

(19) Liu, N.; Song, W.; Wang, P.; Lee, K.; Chan, W.; Chen, H.; Cai, Z. Proteomics analysis of differential expression of cellular proteins in response to avian H9N2 virus infection in human cells. *Proteomics* **2008**, *8* (9), 1851–8.

(20) Vester, D.; Rapp, E.; Gade, D.; Genzel, Y.; Reichl, U. Quantitative analysis of cellular proteome alterations in human influenza A virus-infected mammalian cell lines. *Proteomics* **2009**, *9* (12), 3316–27.

(21) Rescher, U.; Gerke, V. Annexins—unique membrane binding proteins with diverse functions. *J. Cell Sci.* **2004**, *117* (Pt 13), 2631–9.

(22) Futter, C. E.; White, I. J. Annexins and endocytosis. *Traffic* **2007**, *8* (8), 951–8.

(23) Arcangeletti, M. C.; Pinaridi, F.; Missorini, S.; De Conto, F.; Conti, G.; Portincasa, P.; Scherrer, K.; Chezzi, C. Modification of cytoskeleton and prosome networks in relation to protein synthesis in influenza A virus-infected LLC-MK2 cells. *Virus Res.* **1997**, *51* (1), 19–34.

(24) Watanabe, T.; Watanabe, S.; Kawaoka, Y. Cellular networks involved in the influenza virus life cycle. *Cell Host Microbe* **2010**, *7* (6), 427–39.

(25) Pinol-Roma, S. HnRNP proteins and the nuclear export of mRNA. *Semin. Cell Dev. Biol.* **1997**, *8* (1), 57–63.

(26) Rothrock, C. R.; House, A. E.; Lynch, K. W. HnRNP L represses exon splicing via a regulated exonic splicing silencer. *EMBO J.* **2005**, *24* (15), 2792–802.

(27) Vester, D.; Rapp, E.; Kluge, S.; Genzel, Y.; Reichl, U. Virus-host cell interactions in vaccine production cell lines infected with different human influenza A virus variants: a proteomic approach. *J. Proteomics* **2010**, *73* (9), 1656–69.

(28) Bortz, E.; Westera, L.; Maamary, J.; Steel, J.; Albrecht, R. A.; Manicassamy, B.; Chase, G.; Martinez-Sobrido, L.; Schwemmle, M.; Garcia-Sastre, A. Host- and strain-specific regulation of influenza virus polymerase activity by interacting cellular proteins. *mBio* **2011**, *2* (4), No. e00151-11.

(29) Naito, T.; Momose, F.; Kawaguchi, A.; Nagata, K. Involvement of Hsp90 in assembly and nuclear import of influenza virus RNA polymerase subunits. *J. Virol.* **2007**, *81* (3), 1339–49.

(30) Gorg, A.; Weiss, W.; Dunn, M. J. Current two-dimensional electrophoresis technology for proteomics. *Proteomics* **2004**, *4* (12), 3665–85.

(31) Peerschke, E. L.; Ghebrehiwet, B. The contribution of gC1qR/p33 in infection and inflammation. *Immunobiology* **2007**, *212* (4–5), 333–42.

(32) Rao, C. M.; Deb, T. B.; Gupta, S.; Datta, K. Regulation of cellular phosphorylation of hyaluronan binding protein and its role in the formation of second messenger. *Biochim. Biophys. Acta* **1997**, *1336* (3), 387–93.

(33) Ghebrehiwet, B.; Lim, B. L.; Peerschke, E. L.; Willis, A. C.; Reid, K. B. Isolation, cDNA cloning, and overexpression of a 33-kD cell surface glycoprotein that binds to the globular “heads” of C1q. *J. Exp. Med.* **1994**, *179* (6), 1809–21.

(34) Yao, Z. Q.; Shata, M. T.; Tricoche, N.; Shan, M. M.; Brotman, B.; Pfahler, W.; Hahn, Y. S.; Prince, A. M. gC1qR expression in chimpanzees with resolved and chronic infection: potential role of HCV core/gC1qR-mediated T cell suppression in the outcome of HCV infection. *Virology* **2006**, *346* (2), 324–37.

(35) Waggoner, S. N.; Hall, C. H.; Hahn, Y. S. HCV core protein interaction with gC1q receptor inhibits Th1 differentiation of CD4+ T cells via suppression of dendritic cell IL-12 production. *J. Leukocyte Biol.* **2007**, *82* (6), 1407–19.

(36) Yu, L.; Zhang, Z.; Loewenstein, P. M.; Desai, K.; Tang, Q.; Mao, D.; Symington, J. S.; Green, M. Molecular cloning and characterization of a cellular protein that interacts with the human immunodeficiency virus type 1 Tat transactivator and encodes a strong transcriptional activation domain. *J. Virol.* **1995**, *69* (5), 3007–16.

(37) Luo, Y.; Yu, H.; Peterlin, B. M. Cellular protein modulates effects of human immunodeficiency virus type 1 Rev. *J. Virol.* **1994**, *68* (6), 3850–6.

(38) Matthews, D. A.; Russell, W. C. Adenovirus core protein V interacts with p32—a protein which is associated with both the mitochondria and the nucleus. *J. Gen. Virol.* **1998**, *79* (Pt 7), 1677–85.

(39) Beatch, M. D.; Everitt, J. C.; Law, L. J.; Hobman, T. C. Interactions between rubella virus capsid and host protein p32 are important for virus replication. *J. Virol.* **2005**, *79* (16), 10807–20.

(40) Nijtmans, L. G.; de Jong, L.; Artal Sanz, M.; Coates, P. J.; Berden, J. A.; Back, J. W.; Muijsers, A. O.; van der Spek, H.; Grivell, L. A. Prohibitins act as a membrane-bound chaperone for the stabilization of mitochondrial proteins. *EMBO J.* **2000**, *19* (11), 2444–51.

(41) Sharma, A.; Qadri, A. Vi polysaccharide of *Salmonella typhi* targets the prohibitin family of molecules in intestinal epithelial cells and suppresses early inflammatory responses. *Proc. Natl. Acad. Sci. U.S.A.* **2004**, *101* (50), 17492–7.

(42) Ande, S. R.; Mishra, S. Prohibitin interacts with phosphatidylinositol 3,4,5-triphosphate (PIP3) and modulates insulin signaling. *Biochem. Biophys. Res. Commun.* **2009**, *390* (3), 1023–8.

(43) Rajalingam, K.; Wunder, C.; Brinkmann, V.; Churin, Y.; Hekman, M.; Sievers, C.; Rapp, U. R.; Rudel, T. Prohibitin is required for Ras-induced Raf-MEK-ERK activation and epithelial cell migration. *Nat. Cell Biol.* **2005**, *7* (8), 837–43.

(44) Kuadkitkan, A.; Wikan, N.; Fongsaran, C.; Smith, D. R. Identification and characterization of prohibitin as a receptor protein mediating DENV-2 entry into insect cells. *Virology* **2010**, *406* (1), 149–61.

(45) Tsutsumi, T.; Matsuda, M.; Aizaki, H.; Moriya, K.; Miyoshi, H.; Fujie, H.; Shintani, Y.; Yotsuyanagi, H.; Miyamura, T.; Suzuki, T.; Koike, K. Proteomics analysis of mitochondrial proteins reveals overexpression of a mitochondrial protein chaperon, prohibitin, in cells expressing hepatitis C virus core protein. *Hepatology* **2009**, *50* (2), 378–86.

(46) Woo, H. A.; Yim, S. H.; Shin, D. H.; Kang, D.; Yu, D. Y.; Rhee, S. G. Inactivation of peroxiredoxin I by phosphorylation allows localized H<sub>2</sub>O<sub>2</sub> accumulation for cell signaling. *Cell* **2010**, *140* (4), 517–28.

(47) Watanabe, A.; Yoneda, M.; Ikeda, F.; Sugai, A.; Sato, H.; Kai, C. Peroxiredoxin I is required for efficient transcription and replication of measles virus. *J. Virol.* **2011**, *85* (5), 2247–53.

(48) Jamaluddin, M.; Wiktorowicz, J. E.; Soman, K. V.; Boldogh, I.; Forbus, J. D.; Spratt, H.; Garofalo, R. P.; Brasier, A. R. Role of peroxiredoxin 1 and peroxiredoxin 4 in protection of respiratory syncytial virus-induced cysteinyl oxidation of nuclear cytoskeletal proteins. *J. Virol.* **2010**, *84* (18), 9533–45.

(49) Wahl, A.; Schafer, F.; Bardet, W.; Hildebrand, W. H. HLA class I molecules reflect an altered host proteome after influenza virus infection. *Hum. Immunol.* **2010**, *71* (1), 14–22.

(50) Shaw, M. L.; Stone, K. L.; Colangelo, C. M.; Gulcicek, E. E.; Palese, P. Cellular proteins in influenza virus particles. *PLoS Pathog.* **2008**, *4* (6), e1000085.

(51) LeBouder, F.; Morello, E.; Rimmelzwaan, G. F.; Bosse, F.; Pechoux, C.; Delmas, B.; Riteau, B. Annexin II incorporated into influenza virus particles supports virus replication by converting plasminogen into plasmin. *J. Virol.* **2008**, *82* (14), 6820–8.

(52) LeBouder, F.; Lina, B.; Rimmelzwaan, G. F.; Riteau, B. Plasminogen promotes influenza A virus replication through an annexin 2-dependent pathway in the absence of neuraminidase. *J. Gen. Virol.* **2010**, *91* (Pt 11), 2753–61.

(53) van Diepen, A.; Brand, H. K.; Sama, I.; Lambooy, L. H.; van den Heuvel, L. P.; van der Well, L.; Huynen, M.; Osterhaus, A. D.; Andeweg, A. C.; Hermans, P. W. Quantitative proteome profiling of respiratory virus-infected lung epithelial cells. *J. Proteomics* **2010**, *73* (9), 1680–93.

(54) Chase, G.; Deng, T.; Fodor, E.; Leung, B. W.; Mayer, D.; Schwemmle, M.; Brownlee, G. Hsp90 inhibitors reduce influenza virus replication in cell culture. *Virology* **2008**, *377* (2), 431–9.